Spectral measurement using IC-compatible linear variable optical filter

Arvin Emadi[1]*, Semen Grabarnik[1], Huaiwen Wu[1], Ger de Graaf[1], Karin Hedsten[2], Peter Enoksson[2], Jose Higino Correia[3] and Reinoud F. Wolffenbuttel[1]
[1]Delft University of Technology, Faculty of EEMCS, Department of ME/EI, Mekelweg 4, 2628 CD Delft, The Netherlands
[2]MC2, Chalmers University of Technology, SE-412 58, Gothenburg, Sweden
[3]Department of Industrial Electronics, Campus de Azurém, University of Minho, 4800-058 Guimarães, Portugal

ABSTRACT

This paper reports on the functional and spectral characterization of a microspectrometer based on a CMOS detector array covered by an IC-Compatible Linear Variable Optical Filter (LVOF). The Fabry-Perot LVOF is composed of 15 dielectric layers with a tapered middle cavity layer, which has been fabricated in an IC-Compatible process using resist reflow. A pattern of trenches is made in a resist layer by lithography and followed by a reflow step result in a smooth tapered resist layer. The lithography mask with the required pattern is designed by a simple geometrical model and FEM simulation of reflow process. The topography of the tapered resist layer is transferred into silicon dioxide layer by an optimized RIE process. The IC-compatible fabrication technique of such a LVOF, makes fabrication directly on a CMOS or CCD detector possible and would allow for high volume production of chip-size micro-spectrometers. The LVOF is designed to cover the 580 nm to 720 spectral range. The dimensions of the fabricated LVOF are 5×5 mm^2. The LVOF is placed in front of detector chip of a commercial camera to enable characterization. An initial calibration is performed by projecting monochromatic light in the wavelength range of 580 nm to 720 nm on the LVOF and the camera. The wavelength of the monochromatic light is swept in 1 nm steps. The Illuminated stripe region on the camera detector moves as the wavelength is swept. Afterwards, a Neon lamp is used to validate the possibility of spectral measurement. The light from a Neon lamp is collimated and projected on the LVOF on the camera chip. After data acquisition a special algorithm is used to extract the spectrum of the Neon lamp.

Keywords: Microspectrometer, Linear Variable Filter, CMOS-compatible optical sensors, tapered Fabry-Perot

1. INTRODUCTION

Single-chip optical micro-spectrometers have huge potential in many applications, such as identification of bio-molecules, gas detection and in chemical analysis, because of their properties such as low-cost and low sample volume [1]-[5]. A small Linear Variable Optical Filter (LVOF) integrated with an array of optical detectors is a very suitable candidate for a micro-spectrometer that should feature both low unit cost and high resolving power [6]-[7]. Although grating based micro-spectrometers generally outperform optical resonance based systems, such as the Fabry-Perot etalon or the LVOF-based micro-spectrometer, in case of operation over a wide spectral bandwidth, LVOF-based micro-spectrometers are more suitable for operation with high resolving power over a narrow spectral band, as is required in spectral analysis around an absorption line [8]. IC-Compatible fabrication enables the fabrication of LVOFs as a post-process in CMOS. Having the detector array and electronic circuits realized in CMOS prior to application of the post-process offers opportunities for low unit costs in case of a high production volume.

The LVOF is basically a one-dimensional array of many Fabry-Perot (FP)-type of optical resonators. Rather than a huge number of discrete devices [9], the LVOF has a center layer (the resonator cavity) in the shape of a strip and a thickness that changes over its length. Dielectric mirrors are on either side. The spectral resolution of a Fabry-Perot interferometer is determined by surface flatness, parallelism between the two mirror surfaces and mirror reflectivity. The possibility to have high number of spectral channels in a LVOF spectrometer theoretically makes it possible to have spectral

Micro-Optics 2010, edited by Hugo Thienpont, Peter Van Daele, Jürgen Mohr, Hans Zappe,
Proc. of SPIE Vol. 7716, 77162G · © 2010 SPIE · CCC code: 0277-786X/10/$18
doi: 10.1117/12.854548

resolution better than 0.2 nm in the visible spectrum range using signal processing techniques. For a Fabry-Perot type of LVOF, the thickness variation of the cavity layer has to be in order of quarter of the wavelength and very well controlled, which makes fabrication of miniature LVOFs a technological challenge. The theoretical limit for the spectral resolving power of the LVOF-based spectrometer is the spectral bandwidth divided by the number of channels in the detector array. However, this is difficult to achieve when considering the Signal to Noise Ratio. This simple geometric optimum is only approached in case of a high SNR.

LVOF fabrication is based on reflow of a specially patterned layer of resist. Figure 1 shows the process steps for the fabrication of an IC-Compatible LVOF. The process starts with deposition of the lower dielectric mirror stack and the oxide layer that results in the cavity layer. Photoresist is spin coated as the next step and lithography is applied to define the strip-like structure in the resist layer to be reflown. A series of trenches of constant width and with variable spatial frequency or trenches of variable width and constant pitch are etched over the length of the strip of resist to vary the effective amount of resist per unit area. The subsequent reflow transfers this gradient volume of resist into a smooth tapered resist layer. The topography of the tapered resist layer is transformed into the thick oxide cavity layer by an appropriate plasma etching process. The process is completed by deposition of the top dielectric mirror stack. This first prototype of the LVOF is fabricated on a glass substrate. Fabrication directly on a CMOS detector chip as a compatible post-process is well possible and is also demonstrated on small die CMOS chips.

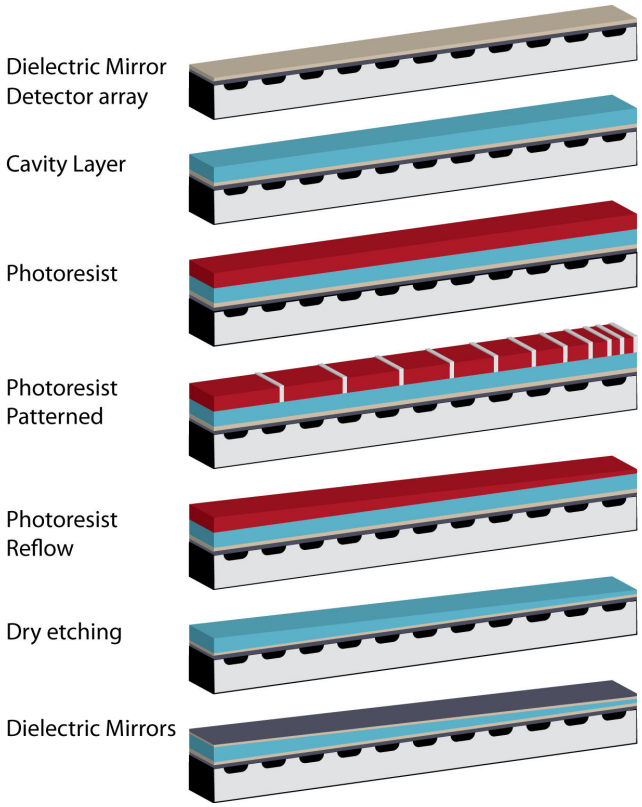

Figure 1. Process flow for fabrication of LVOF.

2. FABRICATION OF LVOF

The LVOF design presented here is designed for operation in the wavelength range between 570 nm and 720 nm. Spectrometers in this wavelength range are suitable for applications such as fluorescence spectroscopy of plants and H-α spectroscopy. The performance characterization of the LVOF and related micro-spectrometer in this wavelength range can be tested using a Neon lamp, which has most of its major peaks in this wavelength range. The same principle of design can be applied to other wavelength ranges in visible, IR and UV. The difference would be in the choice of dielectric materials for the LVOF filter and suitable detector array. For near-infra red region, for example PolySi and SiO_2 are to be used as dielectric materials [10] and MEMS fabricated thermopile arrays as detectors [11].

The dielectric multilayered Fabry-Perot LVOF consists of 15 alternating layers of TiO_2 and SiO_2. Table 1 shows the layers thicknesses required for a visible LVOF to cover the 570 to 720 nm spectral range based on optical simulations. The spectral bandwidth of the filter depends on reflection spectrum of dielectric mirrors and the order of the Fabry-Perot. Increasing the order of the cavity results in higher resolving power, but limits the operating free spectral range of Fabry-Perot etalon. The LVOF based on the Fabry-Perot etalon listed in Table 1 gives a half-power spectral bandwidth HPBW = 2.2 nm over 150 nm wavelength range.

Table 1. Thickness of the layers for visible LVOF

Material	Thickness (nm)
TiO_2	60
SiO_2	102
TiO_2	60
SiO_2	102
TiO_2	60
SiO_2	102
TiO_2	60
SiO_2	800 - 1050
TiO_2	60
SiO_2	102
TiO_2	60
SiO_2	102
TiO_2	60
SiO_2	102
TiO_2	60

Based on the simulation results it was decided to design for 2 types of LVOFs; the first with a length of 2.5 mm and the second with a length of 5 mm. In the 5 mm long LVOF the thickness variation (slope) would be equal to 150 nm / 5 mm.

The first fabrication step of the LVOF is the deposition dielectric mirrors, layers 1 to 7, and a thick oxide of 1050 nm, layer 8, on a 4 inch glass wafer. The thick oxide layer is tapered in subsequent process steps. A FHR MS 150 sputter

machine has been used for deposition of TiO_2 and SiO_2 films. TiO_2 is deposited by reactive DC sputtering and SiO_2 by reactive RF sputtering. The films can be deposited subsequently without breaking the vacuum. The films are optically characterized by ellipsometry and the data were used to refine the values used for the designed thicknesses. The thickness variation over the 4 inch wafer size is measured to be less than 2 % for both films. Thickness variations can cause ± 6 nm wavelength shift of the peak. This implies that fabricating a Fabry-Perot at an exact desired peak can be challenging. For a LVOF type of Fabry-Perot device this problem is resolved, since the sloped cavity layer makes it possible to cover the whole spectrum range of interest despite of wavelength shift. The 4 inch glass wafer is diced into 2 × 2 cm² pieces prior to subsequent processing.

The SiO_2 cavity layer is tapered in an IC-Compatible fabrication process. Initially, a tapered photoresist layer is formed by one step lithography and reflow of the resist. Subsequently, the topography of the tapered resist layer is transferred

into SiO_2 by RIE. With a single lithography step a pattern of trenches (or holes) is developed in a photoresist layer. The trench or holes size is 2 μm, which is the minimum possible with the available lithography. The trench density defines the local amount of material removed and is followed by reflow of this patterned photoresist to locally planarize the remaining strips of material. The result is an effective reduction of the resist layer thickness by a value defined by localized trench density. Hence a taper can be flexibly programmed by mask design to be from 0.001^o to 0.1^o. This enables simultaneous fabrication of tapered layers of different angle. The mask is designed based on a geometrical model and FEM simulations using COMSOL [12]. Figure 2 shows the mask and one patterned photoresist structure before reflow. The mask contains patterns that will result in hill-shaped tapered resist layers of different angles after reflow.

The viscosity of the resist decreases rapidly at temperatures above the glass transition temperature and the material flows because of surface tension, while remaining coherent. Although the glass transition temperature of resist is relatively low value (110 – 120 ºC), the resist does not flow well over the substrate due to its high viscosity. Another approach to decrease the viscosity of the resist is to expose it to its solvent vapor. The samples with patterned resist on the dielectric stack are exposed to PGMEA solvent vapor heated to 50 °C for 3 hours and heated on hotplate at 110 °C for 10 min.

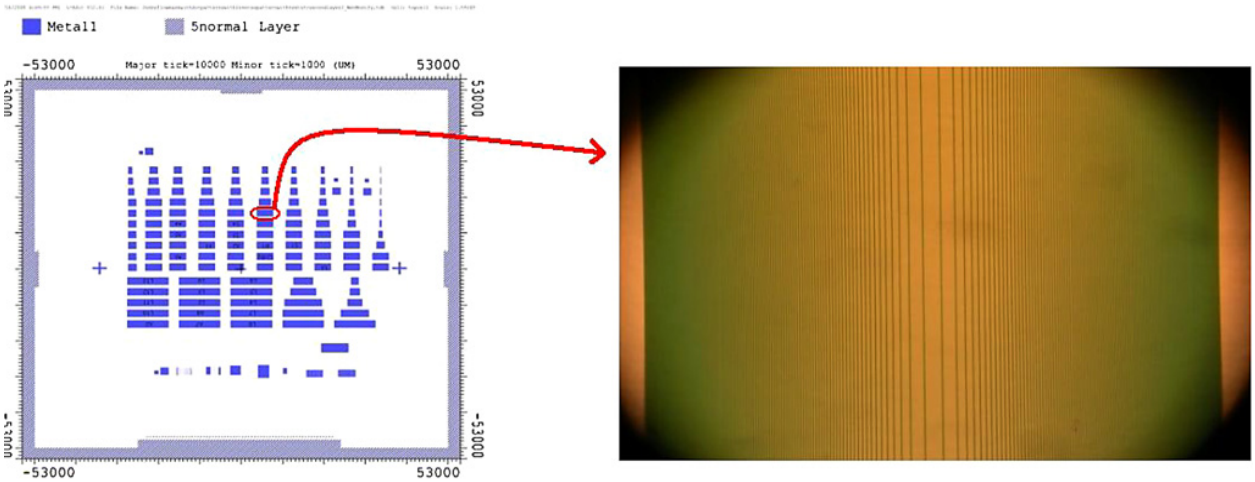

Figure 2. Left) Photo-mask for lithography. Right) patterned photoresist before reflow, trench density increase from the center toward the edges.

The process for transferring the resist structure into SiO_2 is optimized to get an optically smooth surface. The process uses a mixture of NF_3 5 sccm, Ar 50 sccm and O_2 5 sccm at 2 mTorr with 100 Watt. The low chamber pressure will cause the etching process to be slow [13] and result in an acceptable surface roughness of 5 nm on the oxide after etching. The etch rate of the photoresist is 75 nm/min while the etch rate of the SiO_2 is 15 nm/min, which gives a resist/SiO_2 etch ratio of 5. A laser illuminates the thickest part of the resist structure during etching and the reflection from the surface is measured. Due to interference between resist, oxide layer and substrate, this will show exactly how much of the resist and SiO_2 has been etched. The etching process is stopped after resist is removed from the thickest part and 50 nm of the SiO_2 under it, is etched. After etching the samples are cleaned in acetone and further by Oxygen plasma to remove any remaining of photoresist. Subsequently, the dielectric stacks, layers 9 to 15 from table 1, are deposited on the samples to complete the LVOFs. Figure 3 shows the 3D image of one completed LVOF using optical profilometer.

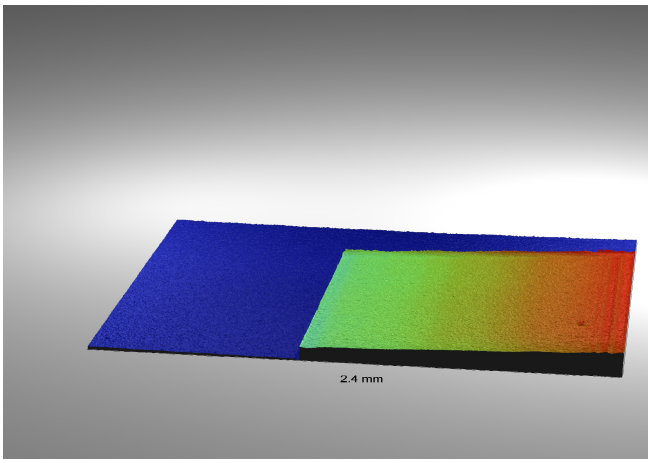

Figure 3. 3D profile of the completed hill-shaped LVOF.

3. CHACTERIZATION AND SPECTRAL MEASUREMENT

The structure of a LVOF based micro-spectrometer is shown in Figure 4. Light passes an aperture and collimating optics before being projected onto the LVOF, which is placed or deposited on the top of the detector. The entrance aperture in figure 4 can be larger than that typically used in grating-based micro-spectrometers, allowing more light entering the optical system. Consequently, the resolution of the micro-spectrometer depends primarily on the Half-Power BandWidth (HPBW) of the LVOF, rather than on the aperture size. To determine the size of aperture and focal length of the collimating lens the following equations can be used:

$d = \frac{D.\varphi}{NA}$ and $f = \frac{D}{2NA}$, In which d is the diameter of the aperture, D is size of the LVOF, f is the focal length of the lens, NA is entrance numerical aperture and φ is maximum acceptable angle of incidence on the LVOF. For spectral resolution better than 2 nm, $\varphi = 5^o$ is an acceptable choice.

In case collimated light of a single wavelength is used to illuminate the LVOF, the light over a small length is transmitted, due to filtering property of the LVOF. The length of the transmitted light spot can be calculated as: $\Delta x = \frac{HPBW}{\theta}$, where θ denotes the slope of the LVOF. Δx is defined as Half Power Line Width (HPLW). Using the values of HPBW=2.2 nm and above mentioned slope angle results in $\Delta x \approx 75\mu m$. This means for each single wavelength in the spectrum a region of 75 μm in length is illuminated on the detector. Therefore, if a typical detector with 5 μm pitch is used, about 15 pixels on the detector are illuminated.

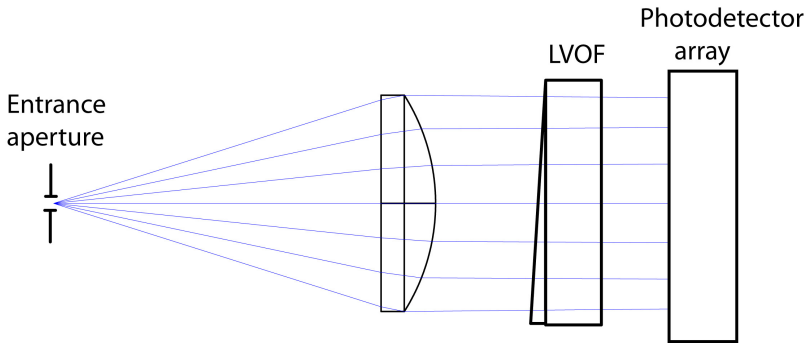

Figure 4. Structure of LVOF micro-spectrometer

The LVOF is mounted on the top of a CMOS camera. A special C-mount lens holder has been fabricated to keep a lens and pinhole for collimation. Figure 5 shows LVOF on a glass substrate mounted on a CCD chip and the C-mount covering them.

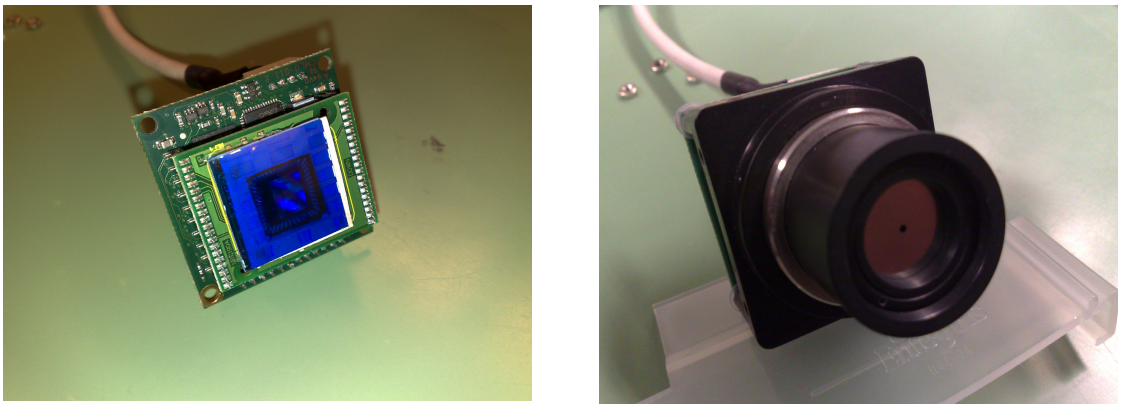

Figure 5. Left) LVOF on glass substrate on the CMOS detector. Right) C-mount lens-pinhole holder on the LVOF and CMOS camera to make the LVOF spectrometer.

In order to do spectral measurement, initially the LVOF spectrometer has to be well calibrated. Collimated light from a monochromater is projected on the LVOF spectrometer and the wavelength is swept from 580 nm to 725 nm with 1 nm steps. Image recorded on the camera is imported to the computer to form the calibration data. Figure 6 shows the recorded image on the camera at several wavelength and intensity profile of the pixels is shown in Figure 7.

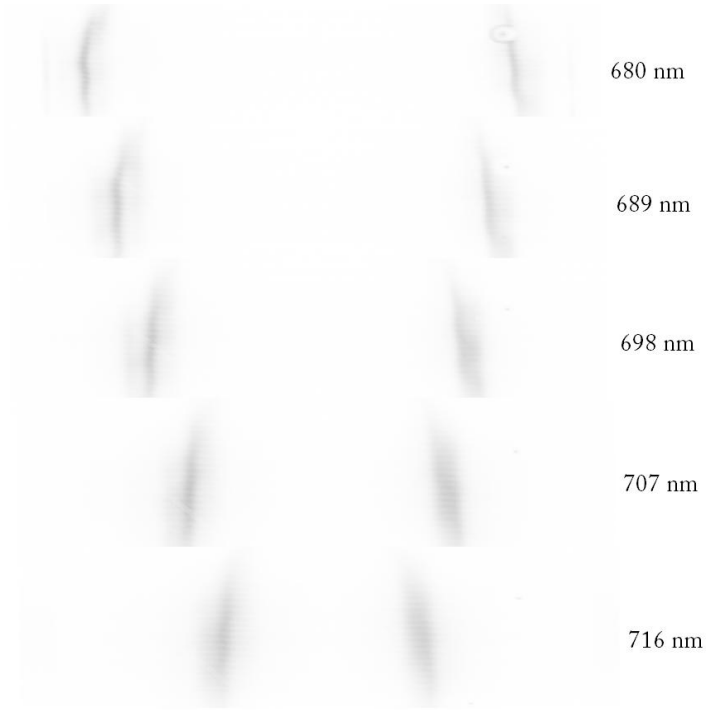

Figure 6. inverted recorded image on the camera at several wavelength

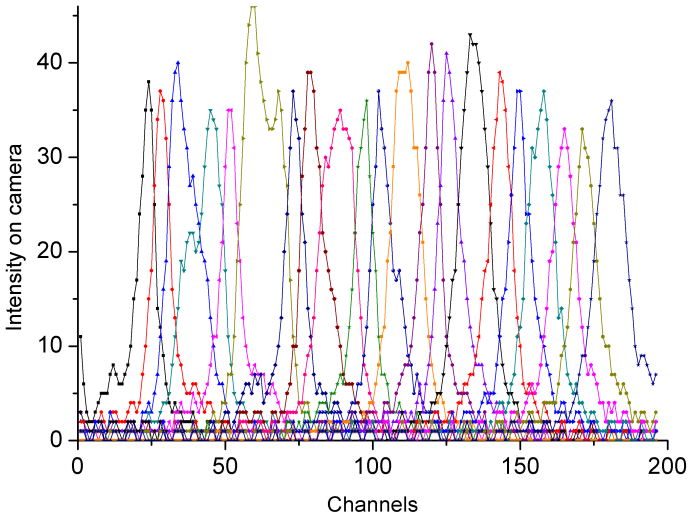

Figure 7. Intensity profile of the camera pixels at 650 – 716 nm spectral range, with 3 nm wavelength steps

Optical ray tracing simulation was carried out using ZEMAX ® software to calculate the image on the camera when illuminated with a Neon lamp. Figure 8 shows the simulated image on the camera and the corresponding intensity profile of the pixels.

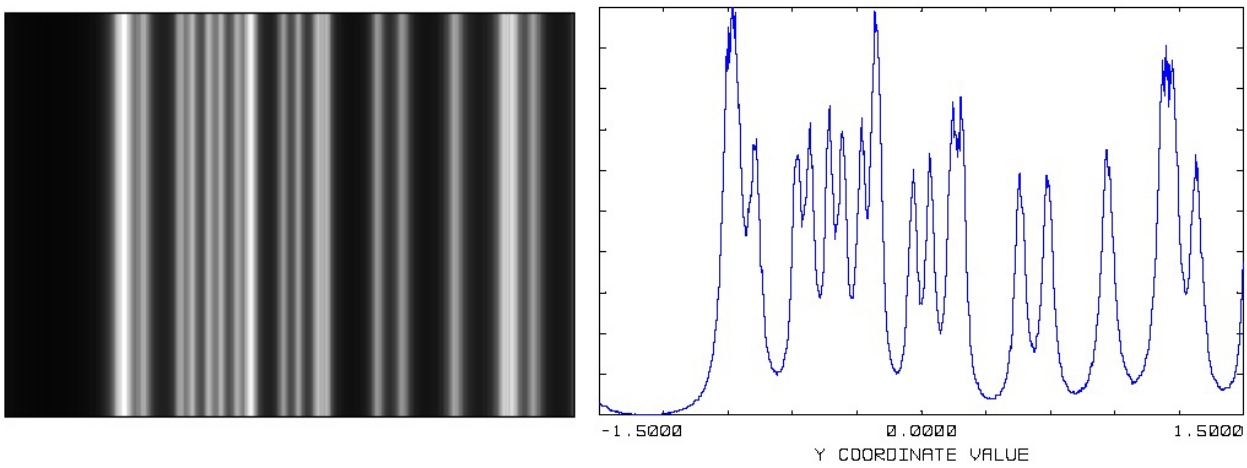

Figure 8. left) simulated image on the lvof spectrometer when illuminated with Neon lamp. Right) simulated intensity profile on the pixels

The simulated intensity profile on the pixels shows the effect of the HPLW. The spectral lines from the Neon lamp widen and result in illuminated stripes with the width of HPLW which will be added together. Calibration data has to be used to separate the spectral lines.

Initially the spectral bandwidth of interest is divided into N spectral channels. The element C_{ij} in matrix C is defined as the intensity of channel i of the detector to component j in the spectrum (i, j = 1...N). Matrix C can be directly formed with the data from calibration measurement. Maximum value of N is the number of the pixels on the camera. Hence, the measured intensity on the detector channels can be described as:

$$\begin{bmatrix} d_1 \\ d_2 \\ \dots \\ d_N \end{bmatrix} = \begin{bmatrix} c_{11} & c_{21} \dots c_{N1} \\ c_{12} & c_{22} \dots c_{N2} \\ \dots & \dots \dots \\ c_{1N} & c_{2N} \dots c_{NN} \end{bmatrix} \begin{bmatrix} I_1 \\ I_2 \\ \dots \\ I_N \end{bmatrix} \text{ or } D_{IN} = C_{NN} * I_{IN}.$$

In which d_i denotes the measured intensity in channel N and I_i denotes the input spectrum intensity that has to be calibrated. For a properly designed and fabricated LVOF, Matrix C has no singularity and it is possible to take the inverse transform of the matrix. Therefore matrix I can be calculated as:

$$\begin{bmatrix} I_1 \\ I_2 \\ \dots \\ I_N \end{bmatrix} = \begin{bmatrix} c_{11} & c_{21} \dots c_{N1} \\ c_{12} & c_{22} \dots c_{N2} \\ \dots & \dots \dots \\ c_{1N} & c_{2N} \dots c_{NN} \end{bmatrix}^{-1} \begin{bmatrix} d_1 \\ d_2 \\ \dots \\ d_N \end{bmatrix} \text{ or } I_{IN} = C_{NN}^{-1} * D_{IN}.$$

However, since the measured matrix D is added with noise the above solution does not give the best answer. An iterative procedure needs to be implemented to calculate matrix I minimizing matrix E,

$$E = \begin{bmatrix} d_1 \\ d_2 \\ \dots \\ d_N \end{bmatrix} - \begin{bmatrix} c_{11} & c_{21} \dots c_{N1} \\ c_{12} & c_{22} \dots c_{N2} \\ \dots & \dots \dots \\ c_{1N} & c_{2N} \dots c_{NN} \end{bmatrix} \begin{bmatrix} \hat{I}_1 \\ \hat{I}_2 \\ \dots \\ \hat{I}_N \end{bmatrix}$$

In which matrix $\hat{I}$ is the estimate of I.

Figure 9 shows the recorded image of the CMOS camera for two LVOF with a different slope when illuminated with Neon lamp. The LVOF image on the left has 250 nm thickness slope and covers the entire spectral band of interest, while the LVOF on the right has 150 nm thickness slope and therefore does not cover the entire band. The intensity profile of the pixels has been used an iterative procedure to estimate $\hat{I}$, however the algorithm did not converge due to too much disturbance in the measurement. The disturbance in the measured matrix of D has three sources: surface roughness of the LVOF, which would cause scattering of the light, insufficient collimation and out of band light. While the first two are expected to be in an acceptable range, it is possible that the Neon lamp used emits light in the infra-red region of the spectrum. To verify this assumption, an infra-red blocking filter of a commercial camera has been put in front the Neon lamp. Figure 10a shows the recorded image. More spectral lines can be observed on the image compared to figure 9. Figure 10b shows the intensity profile of the pixels.

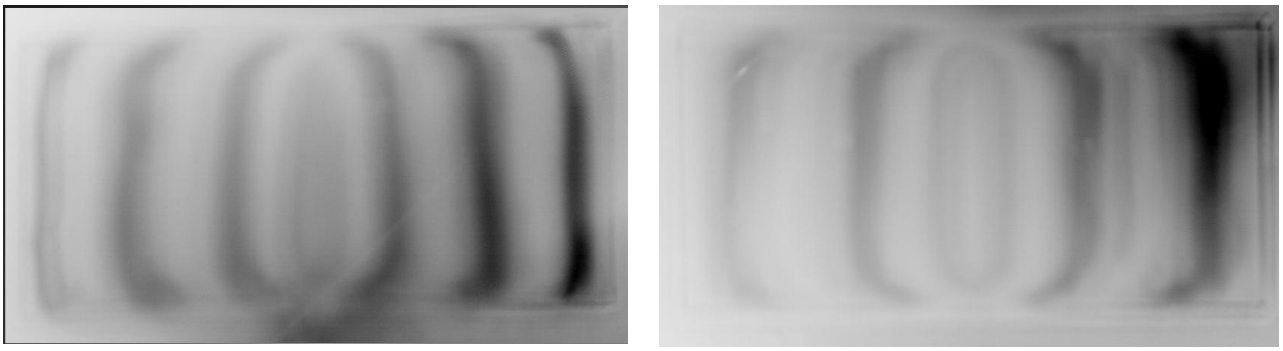

Figure 9. Inverted image of recorded image on the CMOS camera when illuminated with Neon lamp.

Although filtering of the Neon lamp has reduced the disturbance considerably, a comparison between figures 9b and 7 shows that there is still a high level of disturbance in the measurement, which could be further reduced by an improved filtering of the Neon lamp and improved collimation. Moreover, it is necessary to improve the algorithm used to ensure convergence despite the presence of disturbance [14], which are the subjects of future research.

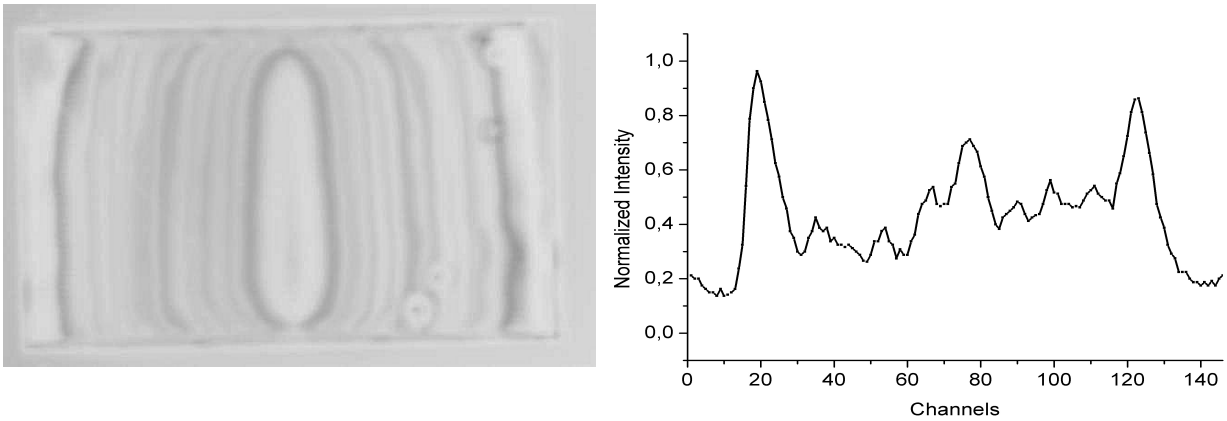

Figure 10. Inverted image of recorded image on the CMOS camera when illuminated with Neon lamp through IR blocking filter.

ACKNOWLEDGMENT

This work has been supported in part by the Dutch technology Foundation STW under grant DET.6667. Part of this work has been done at the Nanofabrication Laboratory of MC2, Chalmers University of Technology, through MC2ACCESS programme.

REFERENCES

[1] G. Minas, R. F. Wolffenbuttel and J. H. Correia. "An array of highly selective Fabry–Perot optical channels for biological fluid analysis by optical absorption using a white light source for illumination, Journal of Optics A: Pure and Applied Optics", IOP Publisher,8, pp.272-278.

[2] J.C. Ribeiro, G. Minas, P. Turmezei, R.F.Wolffenbuttel and J.H. Correia, "A SU-8 fluidic microsystem for biological fluids analysis", Sensors and Actuators A123-124 (2005) pp. 77-81.

[3] G. Minas, R.F.Wolffenbuttel and J.H. Correia, "A lab-on-a-chip for spectrophotometric analysis of biological fluids", RSC Lab Chip, Vol. 5 No. 11, pp. 1303-1309.

[4] S. Grabarnik, R.F. Wolffenbuttel, A. Emadi, M. Loktev, E. Sokolova and G. Vdovin, "Planar double-grating micro-spectrometer", Optics Express, March 19 2007, Vol. 15, No. 6, pp. 3581-3588.

[5] L. Fonseca, R. Rubio, J. Santander, C. Calaza, N. Sabate, P. Ivanov, E. Figueras, I. Gracia, C. Cane, S. Udina, M. Moreno, S. Marco, "Qualitative and quantitative substance discrimination using a CMOS compatible non-specific NDIR microarray", Sensors and Actuators B: Chemical, Volume 141, Issue 2, 7 September 2009

[6] R. McLeod, T. Honda, "Improving the spectral resolution of wedged etalons and linear variable filters with incidence angle", Optics Letters, Vol. 30, No. 19 (2005), pp 2647-2649.

[7] S.F. Pellicori, "Wedge-filter spectrometer", US Patent 4957371

[8] S. Grabarnik, "Optical microspectrometers using imaging diffraction gratings", PhD thesis, Delft University of Technology, ISBN: 978-90-9025048-9

[9] R. Rubio, J. Santander, L. Fonseca, N. Sabate, I. Gracia, C. Cane, S. Udina, S. Marco, "Non-selective NDIR array for gas detection", Sensors and Actuators B: Chemical, Volume 127 (2007), Issue 1, Special Issue: Eurosensors XX, Pages 69-73

[10] A Emadi, S. Grabarnik, H. Wu, G. de Graaf and R. F. Wolffenbuttel. "Fabrication and characterization of infra-red multi-layered interference filter", Proceedings of MME 2007 (2009) (pp. 249-252). Guimaraes,Portugal

[11] H. Wu, S. Grabarnik, A. Emadi, G. de Graaf and R. F. Wolffenbuttel, "A thermopile detector array with scaled TE elements for use in an integrated IR microspectrometer", J. Micromech. Microeng. 18 064017

[12] A Emadi, H. Wu, S. Grabarnik, G. de Graaf and R. F. Wolffenbuttel. "Vertically tapered layers for optical applications fabricated using resist reflow", J. Micromech. Microeng. 19 (2009) 074014 (9pp)

[13] K. Mohamed, M.M. Alkaisi, Three-dimensional pattern transfer on quartz substrates, Microelectronic Engineering, Volume 87, Issues 5-8, The 35th International Conference on Micro- and Nano-Engineering (MNE), May-August 2010, Pages 1463-1466
[14] MASSICOTTE D., MORAWSKI R. Z. BARWICZ A., "Kalman-filter-based algorithms of spectrometric data correction-Part I: An iterative algorithm of deconvolution", IEEE TRANSACTIONS ON INSTRUMENTATION AND MEASUREMENT, Vol. 46, No. 3, June 1997